Improved thermoelectrical properties of Bi-M-Co-O (M=Sr, Ca) misfit compounds by laser directional solidification

J. C. Diez[1], Sh. Rasekh[1], M. A. Madre[1], E. Guilmeau[2], S. Marinel[2], A. Sotelo[1]

(1) Instituto de Ciencia de Materiales de Aragón (ICMA) (CSIC-Universidad de Zaragoza), C/Mª de Luna, 3 50018 Zaragoza. Spain

(2) Laboratoire CRISMAT, UMR 6508 CNRS-ENSICAEN, 6 Boulevard du Maréchal Juin, 14050 CAEN Cedex, France

ABSTRACT

In this work it is reported the improvement of the thermoelectrical properties of bulk samples of composition $Bi_2Sr_2Co_{1.8}O_y$ and $Bi_2Ca_2Co_{1.7}O_y$, when they are properly textured by a directional solidification process, assisted by laser (laser floating zone melting method). Samples composition and microstructure aspects have been studied using X-ray diffraction and scanning electron microscopy. Thermoelectric properties have been measured between 4 and 300K by the simultaneous determination of the electrical resistivity and the thermopower. All the textured samples show a remarkable increase of the power factor values, as compared to the conventional sintered ceramics.

Keywords: thermoelectric oxides, misfit cobaltites, thermoelectric properties, directional solidification, laser floating zone

INTRODUCTION

In response to escalating energy crisis and related pollution problems, we urgently need to adopt new technologies that utilize energy sources in a more efficient and environmentally friendly manner. Thermoelectric power generation has been recognized as one of the innovative and promising energy conservation and environmentally friendly technologies.[1] It allows converting a thermal gradient originated, for example, in exhaust emissions, into an electrical energy output by the well known Seebeck effect. Between other advantages, thermoelectric generation is reliable, clean and silent. On the other hand, big efforts must be still done to obtain more efficient thermoelectric materials and devices.

Since the discovery of a large room temperature thermopower in $NaCo_2O_4$,[2] other layered cobalt oxides, such as Ca-Co-O,[3] Bi-Ca-Co-O,[4] and Bi-Sr-Co-O,[5] have attracted much attention. Their crystal structure is composed of an alternate stacking of a common conductive CdI_2-type CoO_2 layer with a two-dimensional triangular lattice and a block layer, composed of insulating rock-salt-type (RS) layers.[4,6,7] This structure shows a high crystal anisotropy, which is reflected in both, thermoelectric properties as well as a preferential grain growth along the *ab* planes, matching up with the conductive ones.

The performance of a thermoelectric material is evaluated through a dimensionless parameter, the figure of merit ($ZT=S^2T/\rho\kappa$). An easy way for raising this figure of merit is the use of materials with high working temperature. This can be performed by using thermoelectric ceramics, which posses the advantages of higher thermal stability at high temperature and lower toxicity when compared with conventional semiconducting compounds and alloys. In this context, those cobalt oxides seem to be an alternative for thermoelectric power generation devices.

Another way to raise the ZT values for these cobalt oxide families is the improvement of the grain orientation using different techniques. Some of them, involving solid state reactions, have been successfully applied in order to obtain well oriented grains, as hot forging[8] and template grain growth.[9] On the other hand, it is possible to get a

good grain orientation by directional growth from the molten material, as it can be performed by a directional solidification from the melt, induced by laser.[10]

In this paper, we report the main microstructural and thermoelectrical results obtained on $Bi_2Sr_2Co_{1.8}O_y$ and $Bi_2Ca_2Co_{1.7}O_y$ misfit cobaltites textured by a directional solidification process assisted by laser in the same conditions.

EXPERIMENTAL

$Bi_2Ca_2Co_{1.7}O_y$ and $Bi_2Sr_2Co_{1.8}O_y$ polycrystalline samples were prepared by the conventional solid state route using commercial Bi_2O_3 (Panreac, 98 + %), $CaCO_3$ (Panreac, 98 + %), $SrCO_3$ (Panreac, 98 + %), and Co_2O_3 (Aldrich, 98 + %) powders as starting materials. They were weighed in the appropriate proportions, mixed and ball milled for 30 minutes at 300 rpm in an agate mortar. In order to assure the total decomposition of carbonates, the mixed powders were thermally treated twice at 750 and 800ºC for 12h under air, with an intermediate manual milling. This thermal treatment is of the main importance, as it has been designed to decompose the calcium and strontium carbonates, avoiding their presence in the Laser Floating Zone (LFZ) process. Otherwise they would decompose in the melting process, leading to bubble formation inside the liquid phase and, more important, disturbing the crystallization front. The so obtained powders were then isostatically pressed at 200 MPa for 1 minute in order to obtain green cylindrical ceramic bars, which were subsequently used as feed in a LFZ device equipped with a continuous power Nd:YAG solid sate laser (1.06 μm) and described elsewhere.[11]

The texturing processes have been performed downwards with a growth speed of 30 mm/h. In order to assure the compositional homogeneity of the molten zone and maintaining constant the textured rod diameter, the feed has been rotated at 15 rpm. The use of this relatively high crystallization rate implies that the growth process is not produced in a totally equilibrium condition. For this reason, the obtained textured cylinders are formed by the most stable phase, but also accompanied by other phases (secondary phases). In spite of that multiphasic composition, the LFZ process

produces long (more than 20 cm) textured cylinders have been obtained, with c.a. 2 mm diameter. These bars were finally cut to obtain samples having the adequate dimensions for their characterization.

Powder X-ray diffraction (XRD) patterns have been systematically recorded in order to identify the different phases in the thermoelectric textured materials. Data have been collected at room temperature, with 2θ ranging between 10 and 40 degrees, using a Siemens Kristalloflex diffractometer working with Kα Cu radiation.

Microstructures have been observed by scanning electron microscopy JEOL 6000 equipped with an energy dispersive spectroscopy (EDS) device used for phase identification. On the one hand, micrographs of longitudinal fractured sections have been recorded to observe the grain orientation. Longitudinal and transversal polished sections of the samples have been observed to analyze the different phases.

Electrical resistivity measurements were performed longitudinally on textured cylinders using the standard dc four-probe technique at temperatures between 5 and 400K, with no applied external field, in a Physical Properties Measurement System (PPMS) from Quantum Design. Thermopower (TEP or S) measurements were performed at temperatures between 5 and 300K in an experimental setup described elsewhere.[12] With the electrical resistivity and thermopower data, the power factor (PF) has been calculated ($PF = S^2/\rho$) in order to determine the samples thermoelectric performances.

RESULTS AND DICUSSION

XRD has confirmed that the cobaltite phase is the major one, independently of the composition, showing very intense peaks for the (002l) planes. These diffractions indicate that the cobaltite grains have a plate-like shape, with preferential growth along the ab plane. This growth habit is clearly confirmed with the micrograph displayed in Fig. 1, showing a representative fractured longitudinal section of a

textured sample. In this figure, it is possible to observe that grain lengths in the ab plane can easily exceed 100 μm.

The polished longitudinal surfaces of the textured bars are shown in Fig. 2, for the different compositions, where Fig. 2a corresponds to the $Bi_2Ca_2Co_{1.7}O_y$ sample and Fig. 2b to $Bi_2Sr_2Co_{1.8}O_y$. In a first sight, it is clear that the second one is formed by bigger and better oriented grains that the first one. When this figure is analysed more in detail, it is possible to find some more differences between the two compositions. In Fig. 2a, it is possible to distinguish three main different contrasts. A black contrast, with a relatively small size, compared with the other phases, showing a dendritic-like structure, and identified as CoO through EDS analysis. The major phases are the gray ones, which appear with a preferential orientation along the growth direction, and stacked as alternate layers. Dark grey contrast has been associated to the $Bi_2Ca_2Co_2O_y$ cobaltite, while the light grey one is a non thermoelectric phase corresponding to the Bi-Ca-O solid solution. On the other hand, in Fig. 2b it can be observed four different contrasts. As it was indicated for the Ca-containing samples, black phase correspond to CoO and the white phase is identified as the Bi-Sr-O solid solution. Despite the presence of these secondary phases, the samples are mainly composed of highly textured Bi-Sr-Co-O grains alternatively stacked, with compositions $Bi_2Sr_2Co_2O_y$ and $Bi_2Sr_2Co_{1.3}O_y$, and corresponding to the dark and light grey contrasts, respectively. Moreover, the relative proportion of secondary phases is also reduced from the Ca-containing samples (about 35%) to the Sr ones (about 10%), measured as the relative areas of the different phases obtained from SEM micrographs.

The temperature (T) dependence of the resistivity (ρ) of the textured materials, as a function of the composition, is shown in Fig. 3. As it can be easily seen, the ρ(T) curves exhibit a semiconductor-like behaviour from low to high temperature, characterised by a $d\rho/dT < 0$, independently of the nominal composition. This semiconducting behaviour is in agreement with earlier reports on these cobaltite systems.[7,13] The resistivity values decrease from the Ca-containing samples (about 91 mΩ cm at RT) to the Sr ones (about 24 mΩ cm at RT), which are very similar to

the values reported in the literature for these type of materials. These apparently contradictory results for these highly textured materials can be associated to the presence of secondary phases (normally not present in adequately sintered materials), and to a different oxygen content compared to the sintered specimens. On the other hand, a more detailed observation of the graph shows a slight deviation from that behaviour for the Sr-containing samples, between 150 and 250K, where a change on the sign of $d\rho/dT$ is produced, which is in agreement with a more metallic-like behaviour, as it has been previously reported, as a function of the size of the alkaline-earth cation.[14,15] In both cases the samples show a three dimensional Mott variable range hopping (VRH), $\ln \rho \propto T^{-1/4}$ in the low temperature range.

Fig. 4 shows the variation of the thermopower with the temperature as a function of the nominal composition. The sign of the thermopower is positive for the entire measured temperature range, which confirms a mechanism involving holes conduction. The values of the thermopower increase with the temperature, with very similar behaviour in both cases. In the low temperature range (until about 150K), a good agreement with $S \propto T^{1/2}$, which is also described by the three dimensional Mott VRH conduction mechanism. From 150K to room temperature, the S values remain practically constant, as previously reported in this cobaltite family.[16] This more metallic behaviour found for the Sr-containing samples, displayed in resistivity measurements, is confirmed by the lower thermopower values in the plateau-like region. At room temperature, the S values for both samples are about 205 μV/K for the Ca samples and 130 μV/K for the Sr ones, which are higher than those reported in the literature.[6] The high value of the thermopower obtained for these textured bulk materials, prepared by the Laser Floating Zone Melting method, is not common in this system but we can assume that the LFZ growth can probably generate oxygen vacancies in larger content than in bulk samples synthesized in a classic solid state reaction. This reduction on the oxygen content has been confirmed by thermogravimetrical measurements and estimated in around 1-2 wt.%. As a consequence, the carriers concentration (holes) is decreased due to the reduction of the Co^{+4} to Co^{+3} and an increase on the TEP is produced.[15] It has already been

evidenced that, in reduced conditions, the misfit phase $[Ca_2CoO_3][CoO_2]_{1.62}$ is not oxygen stoichiometric but contains considerable amounts of oxygen vacancies.[17]

In order to evaluate the thermoelectric performance of these materials, the power factor, S^2/ρ, has been calculated. The temperature and composition dependences of the power factor (PF) are calculated from the data represented in Figs. 3 and 4, and displayed in Fig. 5. The variation of PF with temperature is similar for both compositions, reaching the maximum values at room temperature, about 0.05 mW/K^2m for the $Bi_2Ca_2Co_{1.7}O_y$ samples, and 0.06 mW/K^2m for the $Bi_2Sr_2Co_{1.8}O_y$ ones, which are higher than the usual values for sintered specimens.

CONCLUSIONS

Microstructural and thermoelectric characteristics of misfit cobaltites, with compositions $Bi_2Sr_2Co_{1.8}O_y$ and $Bi_2Ca_2Co_{1.7}O_y$, directionally grown from the melt by the technique LFZ (laser floating zone) have been studied. The following conclusions can be drawn from the present study:

1. Bulk samples of these misfit cobaltites can be properly grown by the laser floating zone method (LFZ). Highly textured samples with homogeneous dimensions and phase distribution are obtained.

2. Larger and better oriented grains are obtained for the Sr-containing samples. In addition, the amount of secondary phases is lower for these samples.

3. Thermopower values are, in both cases, higher to those found in sintered ceramics. On the other hand, their values are in agreement with the evolution reported in the literature, taking into account the alkaline earth cation size.

4. Electrical resistivity values, in both types of cobaltites, are similar to those obtained for sintered bulk ceramics.

5. An important increase of the power factor (PF) has been obtained in all cases, as a result of raising the thermopower.

6. The use of the laser floating zone (LFZ) melting method seems to be a very useful and promising technique in order to obtain well textured bulk misfit cobaltites with improved thermoelectrical properties.

ACKNOWLEDGEMENTS

The authors wish to thank the Gobierno de Aragón (Project PI154/08 and Research Groups T12 and T74), the Spanish-French Integrated Action (HF2006-0171), and the Spanish Ministry of Science and Innovation (Project MAT2008-00429 and Project CEN 2007-2014) for financial support. The technical contributions of C. Estepa, J. A. Gómez and C. Gallego are also acknowledged.

REFERENCES

1. T. Kajikawa, *J. Electron. Mat.* in press (2009). doi:10.1007/s11664-009-0831-2.

2. I. Terasaki, Y. Sasago and K. Uchinokura, *Phys. Rev B* 56, R12685 (1997). doi: 10.1103/PhysRevB.56.R12685.

3. S. W. Li, R. Funahashi, I. Matsubara, K. Ueno, S. Sodeoka, and H. Yamada, *J. Mater. Chem.* 9, 1659 (1999).

4. A. Maignan, S. Hébert, M. Hervieu, C. Michel, D. Pelloquin, and D. Khomskii, *J. Phys.: Condens. Matter.* 15, 2711 (2003). doi: 10.1088/0953-8984/15/17/323.

5. R. Funahashi, I. Matsubara, and S. Sodeoka, Appl. Phys. Lett. **76**, 2385 (2000). doi: 0003-6951/2000/76(17)/2385/3/$17.00.

6. H. Itahara, C. Xia, J. Sugiyama, and T. Tani, *J. Mater. Chem.* 14, 61 (2004). doi: 10.1039/b309804d.

7. E. Guilmeau, M. Mikami, R. Funahashi, and D. Chateigner, *J. Mater. Res.* 20, 1002 (2005). doi: 10.1557/JMR.2005.0131.

8. V. Garnier, R. Caillard, A. Sotelo, and G. Desgardin, *Physica C* 319, 197 (1999). doi: 10.1016/S0921-4534(99)00308-1.

9. M. M. Seabaugh I. H. Kerscht and C. L. Messing, *J. Am. Ceram. Soc.* 80, 1181 (1997).

10. A. Sotelo, E. Guilmeau, M. A. Madre, S. Marinel, J. C. Diez, and M. Prevel, *J. Eur. Ceram. Soc.* 27, 3697 (2007). doi: 10.1016/j.jeurceramsoc.2007.02.020

11. J. C. Diez, L. A. Angurel, H. Miao, J. M. Fernandez, and G. F. de la Fuente, *Supercond. Sci. Technol.* 11, 101 (1998). doi: 10.1088/0953-2048/11/1/020.

12. J. Hejtmanek, Z. Jirak, M. Marysko, C. Martin, A. Maignan, M. Hervieu, and B. Raveau, *Phys. Rev. B* 60, 14057 (1999). doi: 0163-1829/99/60(20)/14057(9)/$15.00.

13. E. Guilmeau, M. Pollet, D. Grebille, D. Chateigner, B. Vertruyen, R. Cloots, and R. Funahashi, *Mater. Res. Bull.* 43, 394 (2008). doi: 10.1016/j.materresbull.2007.02.043.

14. M. Hervieu, A. Maignan, C. Michel, V. Hardy, N. Creon, and B. Raveau, *Phys. Rev. B* 67 045112 (2003). doi: 10.1103/PhysRevB.67.045112

15. A. Maignan, D. Pelloquin, S. Hebert, Y. Klein, and M. Hervieu, *Bol. Soc. Esp. Ceram. V.* 45, 122 (2006).

16. J. Liu, H. S. Yang, Y. S. Chai, L. Zhu, H. Qu, C. H. Sun, H. X. Gao, X. D. Chen, K. Q. Ruan, and L. Z. Cao, *Phys. Lett. A* 356, 85 (2006). doi: 10.1016/j.physleta.2006.03.016.

17. M. Karppinen, H. Fjellvåg, T. Konno, Y. Morita, T. Motohashi, and H. Yamauchi, *Chem. Mater.* 16, 2790 (2004). doi: 10.1021/cm049493n

FIGURE CAPTIONS

Fig. 1. SEM micrograph of a longitudinal fractured sample ($Bi_2Sr_2Co_{1.8}O_y$), showing the typical orientation of the misfit platelike grains. The arrow indicates the growth direction.

Fig. 2 SEM micrographs of longitudinal polished sections of the textured samples: a) $Bi_2Ca_2Co_{1.7}O_y$ and b) $Bi_2Sr_2Co_{1.8}O_y$.

Fig. 3 Temperature dependence of the electrical resistivity, ρ, for the different compositions: (●) $Bi_2Ca_2Co_{1.7}O_y$ and (◆) $Bi_2Sr_2Co_{1.8}O_y$.

Fig. 4 Temperature dependence of the thermopower, TEP, for the different compositions: (●) $Bi_2Ca_2Co_{1.7}O_y$ and (◆) $Bi_2Sr_2Co_{1.8}O_y$.

Fig. 5 Temperature dependence of the power factor, PF, for the different compositions: (●) $Bi_2Ca_2Co_{1.7}O_y$ and (◆) $Bi_2Sr_2Co_{1.8}O_y$.

Figure

Click here to download high resolution image

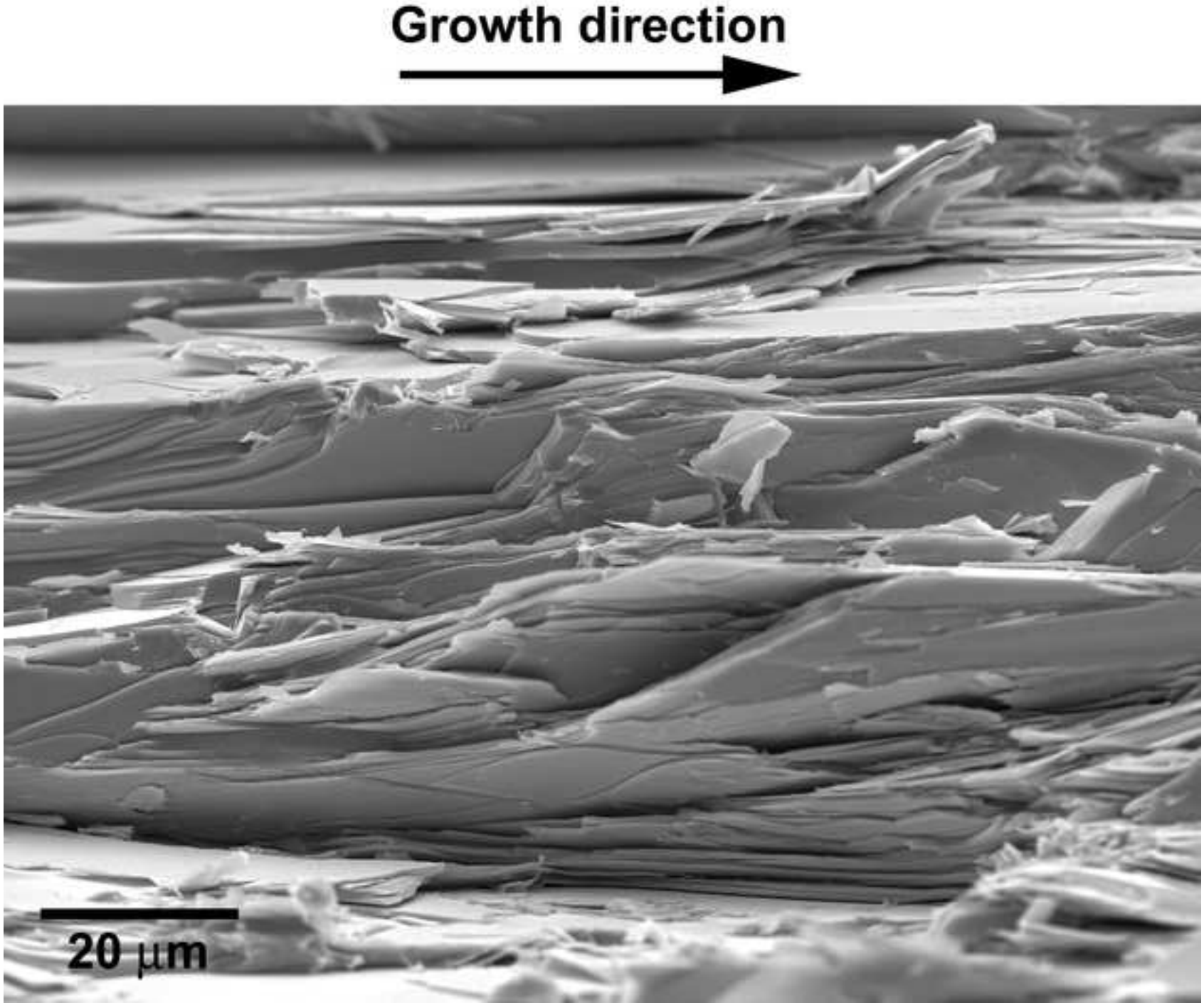

Figure
Click here to download high resolution image

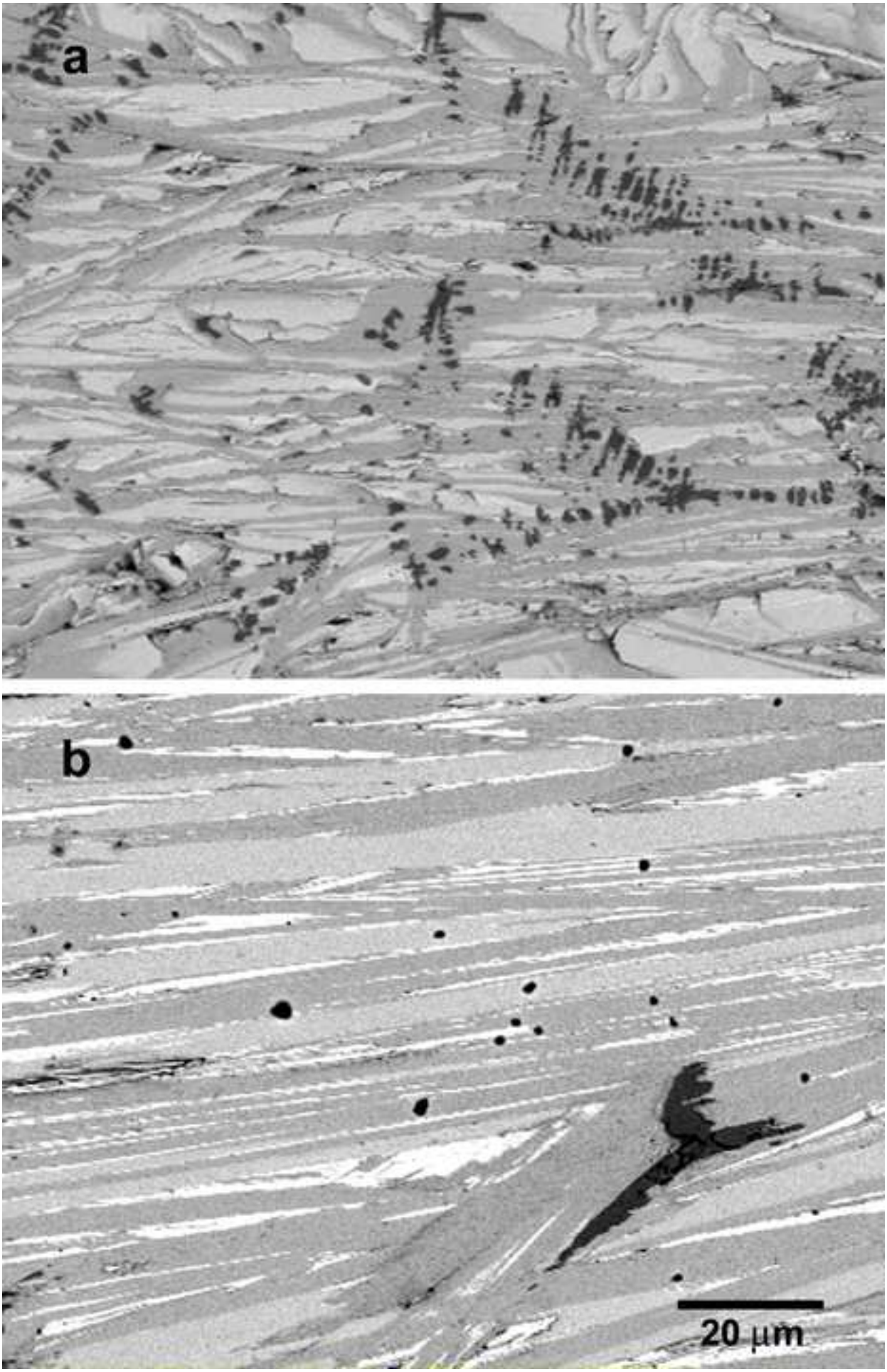

Figure
Click here to download high resolution image

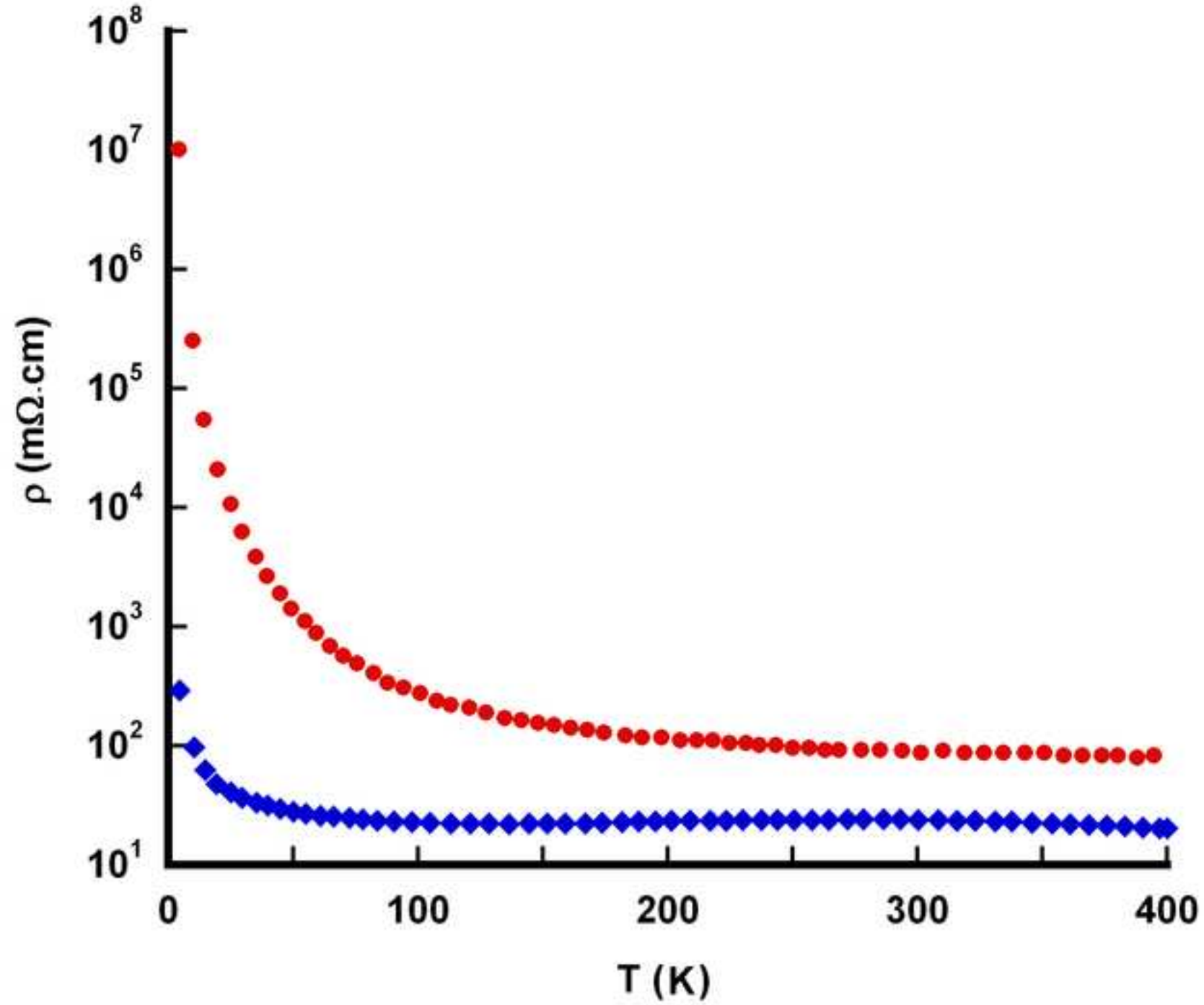

Figure

Click here to download high resolution image

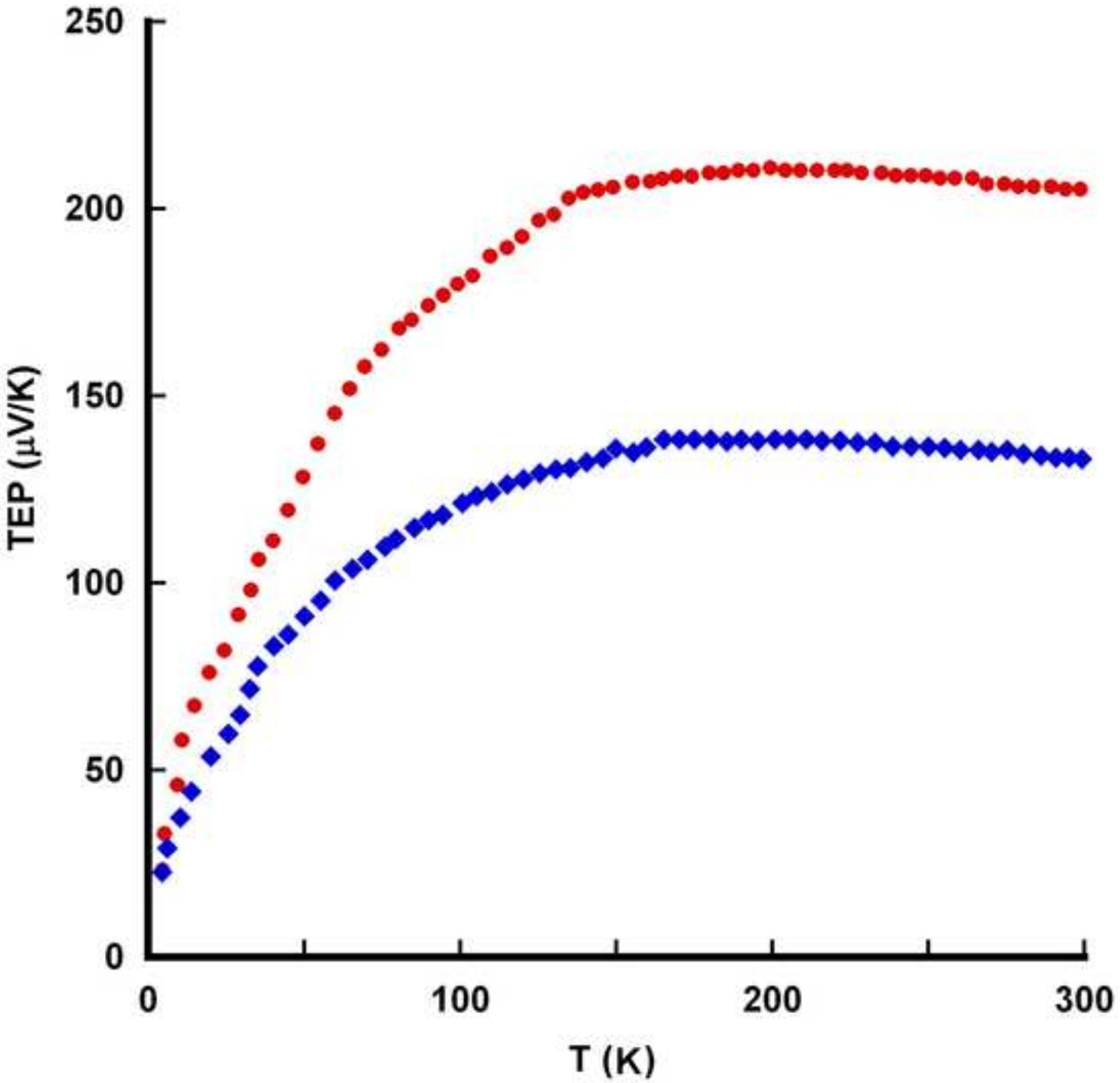

Figure

Click here to download high resolution image